

AN EXPLORATION OF HYDROGEN CONTENT IN MAGNETITE FROM ASTEROID RYUGU. J. Aléon¹, S. Mostefaoui¹, H. Bureau¹, D. Vangu¹, H. Khodja², The Hayabusa2 Initial Analysis Chemistry Team, The Hayabusa 2 Initial Analysis Core. ¹IMPMC, Sorbonne Université, MNHN, CNRS, IRD (61 rue Buffon, 75005 Paris, France, jerome.aleon@mnhn.fr), ²LEEL-NIMBE, CEA, CNRS, Université Paris-Saclay.

Introduction: On December 6 2020, the JAXA space mission Hayabusa 2 returned 5.4 g from the type Cb carbonaceous asteroid Ryugu [1], found to be closely related to Ivuna-type carbonaceous (CI) chondrites [2,3]. The analyzed samples revealed extensive and pervasive aqueous alteration but also exhibit more primitive and reduced characteristics than CI chondrites, which seem to have suffered additional oxidation on Earth [2,3]. Hence, Ryugu provides a unique sampling of hydrated outer solar system material. Because it further escaped oxidation on Earth, the returned Ryugu material offers a unique opportunity to unravel the conditions under which outer solar system water interacted with initially highly unequilibrated material. Magnetite (mgt) is a particularly sensitive tracer of such interactions. Its properties shed light on water-rock ratios, redox conditions or water origin. In Ryugu, it appears to have various morphologies also commonly observed in CI chondrites, such as polyhedral crystals, platelets, fibrous crystals and framboids [3]. Two groups of O isotopic compositions are observed in crystals larger than 5 μm , with $\Delta^{17}\text{O} < 2\%$ in polyhedral mgt and $\Delta^{17}\text{O} \sim 2\text{-}3\%$ in fibrous mgt [2,4]. Synchrotron Mossbauer spectroscopy shows that Ryugu magnetites are fully reduced, whereas they contain excess Fe^{3+} in Orgueil [5]. In order to gain insight on the formation of magnetite and the conditions of aqueous alteration, we developed the measurement of H content in magnetite by NanoSIMS and measured crystals from Ryugu having differing morphology and O isotopic composition.

Samples and methods: 13 mgt crystals (9 polyhedral and 4 fibrous grains) were selected in the polished section A0058-C1001 embedded in epoxy and gold coated, 7 of which (6 polyhedral and 1 fibrous) were previously analyzed for O isotopes by SIMS and characterized by SEM at Hokkaido University [2]. After NanoSIMS analysis, craters were examined using the Tescan Clara FEG-SEM from the MNHN electron microscopy facility to assess the validity of analyses. Several magnetite crystals from the Sorbonne University mineral collection were hand polished, embedded in In, coated with 20 nm C and analyzed for H content by Elastic Recoil Detection Analysis (ERDA) at the nuclear microprobe in LEEL-NIMBE-CEA following established procedures [6] in order to produce suitable standards for determination

of H concentrations. Three mgt samples were found to be homogeneous enough to be used as standards for NanoSIMS analyses, which were conducted with the IMPMC-MNHN NanoSIMS in negative secondary ion mode at 2×10^{-9} Torr. $^{12}\text{C}^-$ or $^{13}\text{C}^-$, $^{16}\text{OH}^-$, $^{18}\text{O}^-$, $^{28}\text{Si}^-$ and $^{56}\text{Fe}^-$ were detected simultaneously on 5 electron multipliers. H contents were measured using $^{16}\text{OH}^- / ^{18}\text{O}^-$ ratios and the calibration established by ERDA on standards. Si contents were estimated semi-quantitatively using the $^{28}\text{Si}^- / ^{56}\text{Fe}^-$ ratio and Si content determined by SEM on the standards.

For crystals $\geq 5 \mu\text{m}$, a 80 pA Cs^+ beam was rastered over 4 μm with blanking so that only the central $2 \times 2 \mu\text{m}$ area was used for analysis. $^{16}\text{OH}^-$, $^{18}\text{O}^-$ and $^{56}\text{Fe}^-$ images acquired before analysis were used to target areas larger than 4 μm adjacent to the Hokkaido O isotopes pits. A 5 min and $10 \times 10 \mu\text{m}$ presputtering was done to reach sputtering equilibrium and ensure minimal contamination. Residual contamination was further monitored by (i) ensuring that the ratios were not affected by changing the raster size and sputtering rates on the standards [7] and (ii) using the $^{13}\text{C}^- / ^{56}\text{Fe}^-$ ratio as a proxy for contamination from organics, due either to the C coat on the standards or to epoxy / indigenous organics on the A0058-C1001 section.

For μm -sized framboids, the primary beam was decreased to 12 pA/170 nm to allow scanning imaging of $8 \times 8 \mu\text{m}$ areas, while at the same time keeping the primary beam as intense as possible to minimize contamination. One standard and a 12 μm Ryugu grain previously analyzed with the 80 pA beam were measured in the same conditions for normalization and comparison. To evaluate H contamination in these conditions the dwell time was varied between 1 ms/pixel and 20 ms/pixel on the standard [7].

Results: The lack of variations with raster size and the lack of correlation with the C/Fe ratio ensured that contamination remained negligible during most analyses performed with the 80 pA beam. Only the smallest fibrous grain (grain 12) had an elevated C signal. With the 12 pA beam, the secondary ion intensities are dominated by topography effects but large enough flat areas (0.6-1 μm wide) were found in the largest framboids. The OH/O ratios were consistently higher by a factor ~ 3 to 5 than those obtained with the 80 pA beam indicating either contamination or a difference in the secondary ion yields due to the measurement conditions. More

investigations are required for a robust determination of H content in frambooids.

Two groups of H contents were found in coarse-grained mgt, correlated with morphology, Si content and O isotopes (Fig. 1). Polyhedral crystals, 6 of which having $\Delta^{17}\text{O} \sim 0\%$, were found to be the most Si-poor and have tightly grouped H contents between 800 and 1500 wt ppm H_2O . By contrast, fibrous grains, 1 of which having $\Delta^{17}\text{O} = +3.1\%$, have higher Si content and have H content ranging from 1300 up to 3500 wt ppm H_2O . Among these, grain 12 with the highest C signal has the lowest H content. Duplicate measurements of 4 polyhedral and 1 fibrous grains yielded consistent results. Examination of NanoSIMS crater pits by FEG-SEM shows that polyhedral mgt remained unchanged during sputtering with smooth morphology, whereas fibrous mgt became highly porous with significant topography upon sputtering, revealing nanoscale heterogeneities possibly due to crystal size or porosity, also observed by TEM [8] or to nano-inclusions.

Discussion and conclusions: The higher $\Delta^{17}\text{O}$ values and H content of fibrous mgt are indicative of precipitation in different aqueous conditions than polyhedral mgt. In section A0058-C1001, the latter is associated with coarse-grained phyllosilicates, whereas fibrous mgt is associated with the fine-grained matrix and frambooids. If the measurements of frambooids can be trusted, the frambooids probably also have high H content. Note that in a CI IDP, mgt frambooids also have $\Delta^{17}\text{O} \sim +2\%$ [9]. This suggests that magnetite has recorded several episodes of aqueous fluid circulations in different conditions possibly with fluids of differing origin. Magnetite may have recorded the evolution of the water-rock ratio during alteration with water being isotopically buffered by the silicate matrix as alteration progresses. In this case, fibrous mgt would have crystallized first, at higher water-rock ratios, in presence of a less equilibrated fluid. This is consistent with carbonates, where calcite has larger $\Delta^{17}\text{O}$ values than dolomite and is estimated to have precipitated first [10]. The higher Si content associated with nanoscale heterogeneity in fibrous mgt may suggest that the higher H content could result from trapping of hydrated nano-silicates during rapid growth rather than higher H content within the crystalline network. This may indicate a dynamic environment with fluid flow for fibrous mgt, while polyhedral mgt would have crystallized in isolated pockets buffered by silicates and acting as a closed-system. More work is clearly required for a better understanding of magnetite formation in CI chondrites and asteroid Ryugu and its implication for aqueous circulations.

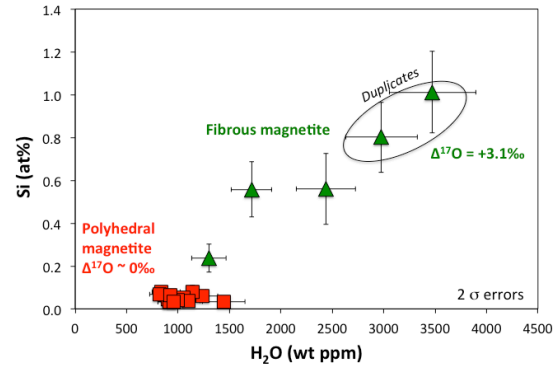


Figure 1: H content expressed as equivalent water content as a function of Si content in magnetite (squares: polyhedral mgt, triangles: fibrous mgt).

The Hayabusa2 Initial Analysis Chemistry

Team: T. Yokoyama, K. Nagashima, I. Nakai, E. D. Young, Y. Abe, C. M. O'D. Alexander, S. Amari, Y. Amelin, K. Bajo, M. Bizzarro, A. Bouvier, R. W. Carlson, M. Chaussidon, B. -G. Choi, N. Dauphas, A. M. Davis, T. Di Rocco, W. Fujiya, R. Fukai, M. K. Haba, Y. Hibiya, H. Hidaka, H. Homma, P. Hoppe, G. R. Huss, K. Ichida, T. Iizuka, T. R. Ireland, A. Ishikawa, S. Itoh, N. Kawasaki, N. T. Kita, K. Kitajima, T. Kleine, S. Komatani, A. N. Krot, M. -C. Liu, Y. Masuda, K. D. McKeegan, M. Morita, K. Motomura, F. Moynier, A. Nguyen, L. R. Nittler, M. Onose, A. Pack, C. Park, L. Piani, L. Qin, S. S. Russell, N. Sakamoto, M. Schönbächler, L. Tafla, H. Tang, K. Terada, Y. Terada, T. Usui, S. Wada, M. Wadhwa, R. J. Walker, K. Yamashita, Q. -Z. Yin, S. Yoneda, H. Yui, A. -C. Zhang, H. Yurimoto.

The Hayabusa2 Initial Analysis core:

S. Tachibana, T. Nakamura, H. Naraoka, T. Noguchi, R. Okazaki, K. Sakamoto, H. Yabuta, H. Yurimoto, Y. Tsuda, S. Watanabe.

Acknowledgements: We thank the Sorbonne University mineral collection for the loan of magnetite standards and S. Pont for help with the MNHN FEG-SEM.

References: [1] Yada T. et al. (2022) *Nat. Astron.* 6, 214-220. [2] Yokoyama T. et al. (2022) *Science*, 10.1126/science.abn7850. [3] Nakamura T. et al. (2022) *Science*, 10.1126/science.abn8671. [4] Kita N. T. et al. (2022) Hayabusa symposium abstract. [5] Viennet J.-C. et al. (2022) LPSC 53, Abstract #1834. [6] Bureau H. et al. (2009) *GCA* 73, 3311-3322. [7] Levy D. et al. (2019) *Anal. Chem.* 91, 13763-13771. [8] Dobrica E. et al. (2022) LPSC 53, Abstract #2188. [9] Aléon J. et al. (2009) *GCA* 73, 4558-4575. [10] Fujiya W. et al. (2022) Hayabusa symposium abstract.